

# POLARIZED POSITRON SOURCE WITH A COMPTON MULTIPLE INTERACTION POINT LINE

I. Chaikovska\*, R. Chehab, O. Dadoun, P. Lepercq, A. Variola

Laboratoire de l'Accélérateur Linéaire (LAL), Université Paris-Sud XI, Orsay, France

## Abstract

Positron sources are critical components of the future linear collider projects. This is essentially due to the high luminosity required, orders of magnitude higher than existing ones. In addition, polarization of the positron beam rather expands the physics research potential of the machine. In this framework, the Compton sources for polarized positron production are taken into account where the high energy gamma rays are produced by the Compton scattering and subsequently converted into the polarized electron-positron pairs in a target-converter. The Compton multiple Interaction Point (IP) line is proposed as one of the solutions to increase the number of the positrons produced. The gamma ray production with the Compton multiple IP line is simulated and used for polarized positron generation. Later, a capture section based on an adiabatic matching device (AMD) followed by a pre-injector linac is simulated to capture and accelerate the positron beam.

## INTRODUCTION

Polarized positron source based on the Compton scattering is one of the attractive methods to produce polarized positrons in the case of the future linear collider projects such as the ILC and CLIC [1]. A general layout of this scheme is shown on Fig. 1. Polarized laser photons are scattered off the electron beam producing the high energy polarized gamma rays. The later is directed to the target-converter resulting in the production of the polarized positrons which are collected and accelerated by Accelerating Capture Section (ACS) consisting of the matching device to capture the produced positrons and the pre-injector linac for primary acceleration. Then, the positron beam is further accelerated and injected in a Damping Ring (DR).

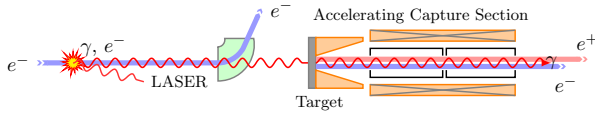


Figure 1: A fundamental scheme of the polarized positron production by the Compton scattering.

The main advantages of the Compton scheme are that the positron source is imposed independently with respect to the main linac and the required drive electron beam energy is much lower as compared with the undulator scheme. However, it suffers from the relatively low value of the scat-

tering cross section resulting in the low number of positrons produced per one electron beam crossing.

Eventually, the challenge of the Compton based Positron Source (CPS) is that, despite the low value of the cross section, to have enough gamma rays to produce enough positrons per second, that is  $\sim (1 - 3) \times 10^{14} e^+ s^{-1}$  as required by the CLIC and ILC. To meet the requirements imposed by these future projects, one needs to increase significantly the flux of the gamma rays produced. This can be done by using a high average power laser system based on a Fabry-Perot cavity and a high current electron beam. Another solution that should allow an important increase of the emitted gamma ray flux is to design a Compton multiple IP line. This requires a system of focusing triplets to focalise the electron beam on each IP.

## POSITRON PRODUCTION WITH COMPTON SCATTERING

### Gamma rays production

There are three types of the CPS according to the electron source used for the Compton scattering: linac based, storage ring based and Energy Recovery Linac (ERL) based CPS. The ERL scheme for CPS is very attractive since the electron bunch after the interaction with the laser pulses is renewed. This allows to have a not degraded bunch for the Compton collisions in every turn which is quite important especially in the case of multiple IP line [3]. Therefore, for this study we consider the CPS is composed of the ERL generating the electron beam followed by the ACS. The parameters of the Compton IP used for the simulations are summarized in Table 1.

Table 1: Compton IP parameters

Description	Value
Electron energy, $E_e$	2 GeV
Electron bunch charge, $C_e$	0.5 nC
Electron bunch length, $\tau_e$	3 ps
Electron IP $\beta_x/\beta_y$	0.1 m/rad
RMS energy spread, $\delta_E$	0.002
Electron emittance, $\gamma\epsilon_x/\gamma\epsilon_y$	10 $\mu\text{m}$ rad
Electron IP beam size, $\sigma_x/\sigma_y$	16 $\mu\text{m}$
LASER photon energy, $E_{ph}$	1.17 eV
LASER beam waist, $\omega_L = 2\sigma_L$	30 $\mu\text{m}$
LASER pulse length, $\tau_L$	5 ps
LASER pulse energy, $E_L$	0.6 J
Crossing angle, $\theta$	2°
Length of one IP, $L_{IP}$	5.4 m

\* chaikovs@lal.in2p3.fr

The simulations of the Compton multiple IP line are done inside a code CAIN [4] and show a good increasing of the gamma ray flux ( see Fig 2). From Fig. 2 one can see also that after a few IPs, chromatism of the electron beam caused by the electron energy spectrum degradation due to the Compton collisions (so-called Compton recoil  $E_{CR}$ ) start to reduce the gain. The effect is magnified by the losses due to the collimation system of the gamma rays installed to reach the degree of polarization required.

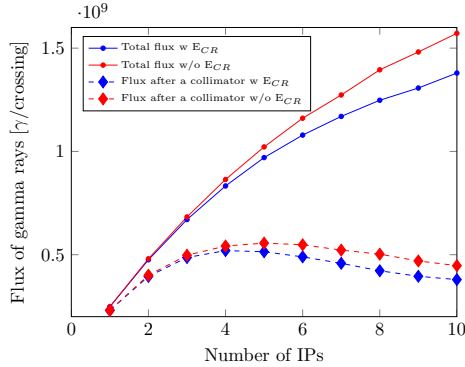


Figure 2: Total gamma ray flux and gamma ray flux obtained after the collimator as a function of the number of the Compton IPs.

It is still efficient to consider 5 IPs where we assumed two lasers cross symmetrically in respect to the beam propagation axis. In this case a factor four of gain is obtained. The further optimization of the focusing quadrupole triplets should be done. The energy spectrum of the gamma rays

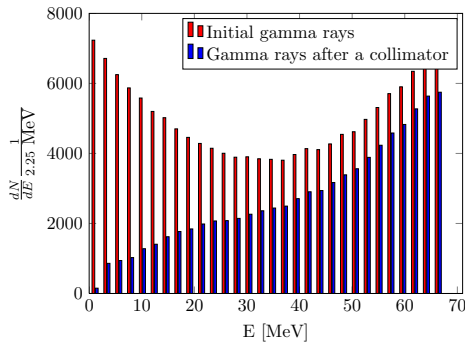


Figure 3: Energy spectrum of the gamma rays produced using the 5 IPs line. .

produced after the 5 IPs is shown on Fig. 3 together with the spectrum selected by the collimator to be used for positron generation. The gamma ray mean energy after the collimator is 45 MeV while the gamma ray polarization equals to 37.9%.

### Target simulation

Simulations of the positron production is performed using a Geant4 code [2] developed at LAL. After the opti-

mization studies regarding the positron yield and polarization, a 4 mm thick target made of Tungsten have been used to produce the polarized positrons. The resulting positron energy spectrum is shown on Fig. 4. The output of this simulation have been used as an input data for the ACS simulation.

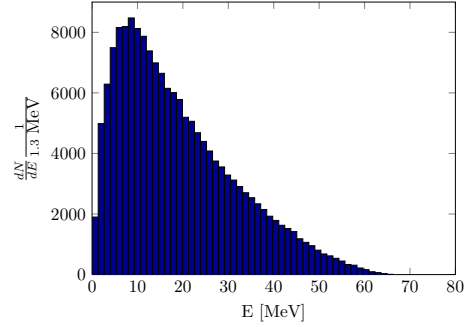


Figure 4: Energy spectrum of the positrons at the exit of the target.

### Accelerating Capture Section

The ACS section is presented by the AMD as the matching device and 2 GHz pre-injector linac made of the 17 MV/m constant gradient Travelling Wave (TW) structures to accelerate the positrons up to the 200 MeV. The simulation of the ACS is performed using a tracking code ASTRA [5].

The AMD is made of the tapered solenoid field and used to match the positron beam after the production to the acceptance of the pre-injector linac. This can be observed in Fig. 5. A positron transverse emittance is transformed in the AMD in such a way that large transverse divergence of the positron beam is decreased and further compressed by the accelerating cavities. The AMD used in the simulation is 20 cm long with a longitudinal magnetic field starting at 6 T and adiabatically decreasing down to 0.5 T. The aperture radius of the AMD is 20 mm. The advantage of using the AMD to quarter wave transformer (QWT) as a matching device is that it allows increase the accepted positron yield by capturing the positrons within a wide energy band.

At the end of the AMD a six 2 GHz TW structures of the pre-injector linac are installed. Each such RF structure is made of 84 cells and 2 couplers with the total length of 4.36 m. The iris radius of the RF cavities is 20 mm. A drift between the structures is set to one  $\lambda_{RF}$  that is about 15 cm. The whole pre-injector linac is encapsulated inside a solenoid with the axial magnetic field equals to 0.5 T. It is employed to avoid the positron losses caused by the high divergence of the positron beam at the beginning of the ACS.

## RESULTS AND DISCUSSION

To define the CPS efficiency, a window with ( $\pm 10$  MeV,  $\pm 10$  mm) around the highest density of

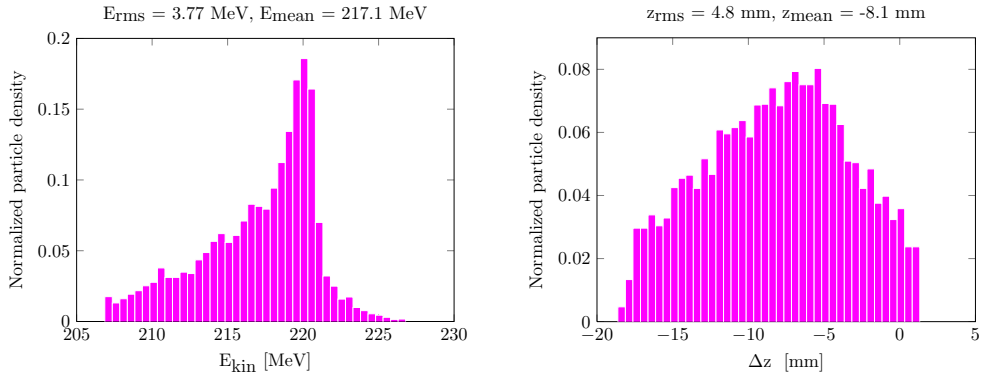


Figure 6: Longitudinal distributions of the positrons at the end of the ACS inside the ( $\pm 10$  MeV,  $\pm 10$  mm) window.

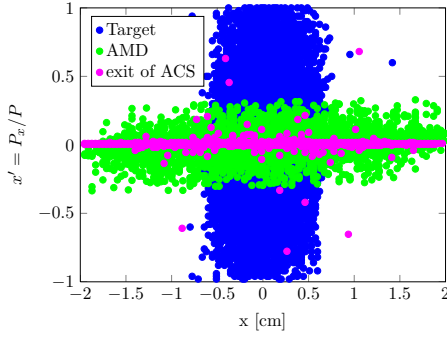


Figure 5: Positron beam emittance taken at the exit of the target, at the exit of the AMD and at the end of the ACS.

positrons is set at the end of the ACS. The longitudinal distributions of the positrons selected by this window is shown on Fig. 6. The main results of the CPS simulation are presented in Table 2. According to them, the CPS efficiency normalized by the electron bunch charge and the energy of the laser pulse in the 5 IPs with two crossed lasers scheme is estimated to be  $1.71 \times 10^{-2}/(\text{nC}\cdot\text{J})$  or  $5.32 \times 10^7 e^+/(\text{nC}\cdot\text{J})$ . A low positron charge produced per bunch can be compensated by the multiple injections in the same DR RF bucket. In the case of the CLIC requirements [6]  $3.72 \times 10^9 e^+$ /bunch, it is equivalent to 70 injections/ $(\text{nC}\cdot\text{J})$ . Assuming the reasonable injection efficiency of 10 injections per DR RF bucket, it is necessary to provide the electron bunches and laser pulses with  $(\text{nC}\cdot\text{J}) \approx 7$  to the the Compton IP what is so far not achievable with the current technologies. However, the different R&D programs are ongoing to improve the performance of the laser systems [7, 8] and to ensure the ERL operation in the nC per bunch range.

## CONCLUSIONS

In the context of the polarized positron sources, we simulated the possible layout of Compton polarized positron source using the multiple IP line. The main positron losses are occurred after the AMD and first TW structure. So,

Table 2: Compton based positron source parameters

Description	Value
Gamma ray production efficiency ( $N_{\gamma}^{tot}/N_{e-}$ )	0.31
Positrons production yield ( $N_{e+}/N_{\gamma}^{ins}$ )	0.2
Mean positron energy at the production	18.9 MeV
Mean positron polarization at the production	35.6%
AMD capture efficiency ( $N_{e+}^{amd}/N_{e+}^{targ}$ )	0.43
Compton source accepted efficiency ( $N_{e+}^{amd}/N_{e-}$ )	0.014
ACS efficiency ( $N_{e+}^{\sim 200\text{MeV}}/N_{e+}^{targ}$ )	0.24
Compton source efficiency ( $N_{e+}^{\sim 200\text{MeV}}/N_{e-}$ )	0.0077
ACS efficiency ( $N_{e+}^{\pm 10\text{MeV} \pm 10\text{mm}}/N_{e+}^{targ}$ )	0.16
Compton source efficiency ( $N_{e+}^{\pm 10\text{MeV} \pm 10\text{mm}}/N_{e-}$ )	0.0051

to improve the CPS efficiency, the further optimizations of the ACS can be done. One of them can imply the tuning the RF phase of the first TW structure to decelerate more the positrons in the first structure and further accelerate them in the following ones. Such technique can allow to capture more positrons and improve the positron bunch characteristics like the energy spread/bunch length what facilitates the stacking of the positrons bunches into the DR.

## REFERENCES

- [1] T. Omori *et al.*, Nucl. Inst. Meth. A500, 232, 2003
- [2] S. Agostinelli *et al.* Geant4: A simulation toolkit. Nucl. Instrum. Meth., A506:250303, 2003
- [3] A. Variola *et al.* In Proceedings of the PAC-2009 IEEE, page MO6RFP068
- [4] K. Yokoya. User manual of CAIN, version 2.40, 2009
- [5] ASTRA: A space charge tracking algorithm, K. Flöttmann, Astra available at <http://tesla.desy.de/~meykopff/>
- [6] A multi-TeV linear collider based on CLIC technology. CLIC Conceptual Design Report (2012)
- [7] J. Bonis, *et al.*, JINST, 7 P01017, IOP Publishing 2012
- [8] T. Akagi, *et al.*, JINST, 7 P01021, IOP Publishing 2012